Linking the uncertainty in simulated Arctic ozone losses to modelling of tropical stratospheric water vapour

Laura Thölix[1], Alexey Karpechko[2], Leif Backman[1], and Rigel Kivi[3]

[1]Climate Research, Finnish Meteorological Institute, Helsinki, Finland
[2]Arctic Research, Finnish Meteorological Institute, Helsinki, Finland
[3]Arctic Research, Finnish Meteorological Institute, Sodankylä, Finland

Correspondence to: L. Thölix (laura.tholix@fmi.fi)

Abstract. Stratospheric water vapour influences the chemical ozone loss in the polar stratosphere via controlling the polar stratospheric cloud formation. The amount of water entering the stratosphere through the tropical tropopause differs substantially between chemistry–climate models (CCM). This is because the present-day models, e.g. CCMs, have difficulties in capturing the whole complexity of processes that control the water transport across the tropopause. As a result there are large differences in the stratospheric water vapour between the models.

In this study we investigate the sensitivity of simulated Arctic ozone loss to the amount of water, which enters the stratosphere through the tropical tropopause. We used a chemical transport model, FinROSE-CTM, forced by ERA-Interim meteorology. The water vapour concentration in the tropical tropopause was varied between 0.5 and 1.6 times the concentration in ERA-Interim, which is similar to the range seen in chemistry climate models. The water vapour changes in the tropical tropopause led to about 1.5 ppm less and 2 ppm more water vapour in the Arctic polar vortex compared to the ERA-Interim, respectively.

We found that the impact of water vapour changes on ozone loss in the Arctic polar vortex depend on the meteorological conditions. Polar stratospheric clouds form in the cold conditions within the Arctic vortex, and chlorine activation on their surface lead to ozone loss. If the cold conditions persist long enough (e.g. in 2010/11), the chlorine activation is nearly complete. In this case addition of water vapour to the stratosphere increased the formation of ICE clouds, but did not increase the chlorine activation and ozone destruction significantly. In the warm winter 2012/13 the impact of water vapour concentration on ozone loss was small, because the ozone loss was mainly NO_x induced. In intermediately cold conditions, e.g. 2013/14, the effect of added water vapour was more prominent, and resulted in 2-7 % more ozone loss than in the colder winters. The results show that the simulated water vapour concentration in the tropical tropopause has a significant impact on the Arctic ozone loss and deserves attention in order to improve future projections of ozone layer recovery.

1 Introduction

Water vapour in the stratosphere is a minor constituent with typical mixing ratios of 3–6 ppmv (e.g., Randel et al., 2004). It plays, however, an important role in radiative and chemical processes. Especially in the upper troposphere/lower stratosphere (UTLS) where changes in the water vapour concentration result in significant changes in radiative forcing of the atmosphere (Riese et al., 2012). A warmer climate in the troposphere increases stratospheric water vapour (SWV) through increases in

the water vapour entering through the tropopause, which warms the climate further (Dessler et al., 2013). Photodissociation of water vapour is an important source of odd hydrogen HO_x (H+OH+HO_2). Catalytic cycles involving HO_x contribute to chemical ozone loss in the stratosphere (Dvortsov and Solomon, 2001). Changes in HO_x affects the chlorine partitioning, which may lead to even more efficient ozone destruction (e.g., Dvortsov and Solomon, 2001). Water vapour contributes to the

5   formation of stratospheric aerosols including polar stratospheric clouds (PSCs), i.e. liquid and solid particles in combination with H_2SO_4 and HNO_3, or ice particles. In addition, the water vapour concentration affects the composition of liquid PSCs, i.e. an increase in water vapour may increase the heterogeneous reaction rates (e.g. Shindell and Grewe (2002)). Heterogeneous reactions in or on PSC particles can lead to massive ozone depletion inside the polar vortices when atmospheric concentration of halogens is sufficiently high (Solomon et al., 1986; Wohltmann et al., 2013). Since the formation of PSCs requires very

10   low temperatures (below about 195 K), significant polar ozone depletion takes place only occasionally in the Arctic (Rex et al., 2006; Manney et al., 2011; Müller et al., 2008; Chipperfield et al., 2015), while it is has been a yearly phenomenon in the Antarctic since about the mid 1980s (Dameris et al., 2014). The stratospheric abundance of chlorine will remain elevated for decades, and polar ozone losses will therefore be seen also in the future. A recovery to 1980 ozone levels will not occur until ca. 2025–2030 in the Arctic and 2050–2070 in the Antarctic (Eyring et al., 2010). Both colder air and increased SWV can

15   increase the formation of PSCs, which could release more active chlorine and cause severe ozone depletion although future chlorine loadings will be smaller. All these suggest that SWV is a critical factor affecting ozone chemistry.

    The majority of the previous studies addressing impacts of SWV on ozone depletion considered the effects of observed (Rosenlof et al., 2001) and projected (Eyring et al., 2007) increases in SWV concentrations (Kirk-Davidoff et al., 1999; Dvortsov and Solomon, 2001; Shindell and Grewe, 2002; MacKenzie and Harwood, 2004; Stenke and Grewe, 2005; Feck

20   et al., 2008; Vogel et al., 2011; Smalley et al., 2017). For example Vogel et al. (2011) used a chemistry–transport model (CTM) and studied the effect of increased SWV on Arctic ozone loss for meteorological conditions from the cold Arctic winter 2004/05. They found that increasing SWV by 0.58 ppm, which is a typical amount simulated by chemistry climate models (CCMs) by the mid-21 century (Eyring et al., 2007), would lead to an additional 6 DU of ozone loss under cold winter conditions. Sinnhuber et al. (2011) used a CTM driven by meteorological conditions for the cold Arctic winter 2010/11 and assumed

25   a uniform increase of SWV of 1 ppm. For such conditions they reported a 25 DU increase in ozone loss, i.e. about 20 % of their simulated total ozone loss for that winter.

    Smalley et al. (2017) studied future trends in the tropical lower stratospheric water vapour and provided a regression model for analysing the factors driving the trends and variability in the 21st-century. They found that warming of the troposphere causes a long term increasing trend in the water vapour entering the stratosphere, which can be partially offset by an increase

30   of the Brewer–Dobson circulation with accompanied cooling of the tropical tropopause. MacKenzie and Harwood (2004) studied the effect of increasing SWV due to future increase in tropospheric methane on ozone. They simulated the year 2060 under the Intergovernmental Panel on Climate Change Special Report on Emission Scenarios (SRES) B2 scenario, where CH_4 lies approximately midway between the extremes of the SRES scenarios. They found an increase in the occurrence of PSCs, with about 20 to 25 % of the increase due to increases in the water vapour. The rest is from radiative cooling of the middle

35   atmosphere due to changes in the concentration of several trace gases. In the simulations by MacKenzie and Harwood (2004)

the increased SWV due to projected methane increases caused a 15 % (about 0.5 ppm at 465 K level) deeper Arctic ozone loss in 2060. However, cooling of the stratosphere could at least partially offset the effect of the increased PSCs by slowing down some gas-phase reactions involved in the catalytic ozone loss cycles (e.g., Revell et al., 2012).

Also Revell et al. (2016) studied the effect of future methane changes on SWV under different RCP-scenarios. The contribution of methane to the SWV was found to be highly dependent on the projected methane concentration, altitude and latitude. Under RCP 6.0 between 1960 and 2100 the SWV was projected to increase by approximately 1 ppm throughout most of the stratosphere, excluding the Antarctic lower stratosphere. The largest increase was seen following the RCP 8.5, with 60 % additional water vapour in the extratropical upper stratosphere, and ca. 35 % in the Arctic lower stratosphere. The largest contribution from methane to the SWV change was about 50 % under RCP 8.5, which assumes a rather extreme methane increase scenario, and the smallest about 4 % under RCP 2.6.

Recently Sagi et al. (2017) studied Arctic ozone losses between years 2002 and 2013 using data assimilation of Odin/Sub-Millimetre Radiometer (SMR) atmospheric observations. They found that the largest ozone losses were caused either by halogens or by the NO_x-family, and the dominating process for ozone destruction is determined mostly by the temperatures inside the polar vortex. The very stable and cold polar vortex in the Arctic winter 2010/11 led to remarkable halogen driven ozone loss with 2.1 ppm ozone destroyed at the 450 K level. In the winter 2012/13 the polar vortex was more unstable and a vortex split occurred early January due to a sudden stratospheric warming (SSW). Thus NO_x rich air from the mesosphere descended to the upper stratosphere and led to ozone loss there. It is therefore likely that the effect on Arctic ozone depletion from changes in SWV will depend on the meteorological conditions, and the dynamical stability in a given winter.

The main source of SWV is the upward transport from the troposphere through the tropical tropopause in the upwelling branch of the Brewer–Dobson circulation. The concentration of SWV is controlled by the coldest temperature met by the ascending air parcels (i.e. cold point temperature). Gettleman et al. (2010) analysed 16 state-of-the-art CCMs and demonstrated large discrepancies between simulated SWV in these models, which were closely related to the simulated cold point temperatures. The 'entry' value of SWV in these models ranged between 2 and 6 ppm, compared to the observed value of 3–4 ppm. These intermodel differences by far exceed the magnitude of the projected water vapour increases in the 21 century used so far in the studies of ozone loss sensitivities to SWV. One may wonder what are the implications of these discrepancies for stratospheric ozone losses simulated by the CCMs? This question is difficult to address by analyzing CCM outputs because there are other differences between the models which affect simulated ozone losses, such as differences in transport. Therefore a more controlled experiment is needed in order to assess the impacts of these SWV differences for ozone losses.

In this study we address the question of what the implications of the differences in simulated tropical stratospheric water vapour between chemistry–climate models are for the simulated Arctic ozone loss. Similar to Vogel et al. (2011) and Sinnhuber et al. (2011) we address this question by performing CTM simulations using different SWV concentrations. The principal differences in our methodology from the previous studies are (1) the boundary conditions of perturbed water vapour experiments resulting in a different spatial pattern of SWV anomalies and (2) the magnitude of SWV perturbation, which is larger than in the Vogel et al. (2011) and Sinnhuber et al. (2011) studies, but in the range of Revell et al. (2016) and MacKenzie and

Harwood (2004). We also analysed seven different winters, whose dynamical circumstances such as the as the evolution of the temperature and polar vortex were different (see Section 3 for more details).

2 Modelling and data

A global off-line chemistry–transport model for the middle-atmosphere, FinROSE-CTM, was used for simulating the effect of the SWV on Arctic ozone depletion. The FinROSE-CTM is described in detail in Damski et al. (2007b). In this study, the model has a horizontal resolution of $3° \times 6°$ (latitude × longitude). It has 40 hybrid-sigma levels up to $0.1\,\mathrm{hPa}$ (about $65\,\mathrm{km}$). The temperature, winds and surface pressure are from the European Centre for Medium-range Weather Forecasts (ECMWF) ERA-Interim reanalyses (Dee et al., 2011).

The model transport is computed using a flux-form semi-lagrangian transport code (Lin and Rood, 1996). The chemistry scheme of the model comprises 36 species and includes about 150 reactions. In addition to gas-phase chemistry, the model includes a PSC scheme with liquid binary aerosols (LBA), supercooled ternary solution of sulfuric acid, nitric acid and water (STS, type Ib), solid nitric acid trihydrate (NAT, type Ia) and ice (ICE, type II) PSCs. The heterogeneous chemistry includes altogether 30 reactions and is based on the calculation of the composition and volume of sulphate aerosols and PSCs, as well as the partitioning of species between gas phase and condensed phase. The number density profile is prescribed for each PSC type (Damski et al., 2007b) and the sulphuric acid distribution is based on 2-D model data (Bekki and Pyle, 1992). Absorption cross-sections and rate coefficients follow the recommendations by Sander et al. (2011) and for some heterogeneous chemistry reactions the recommendations by Atkinson et al. (2007), see details in Damski et al. (2007b). Photodissociation coefficients were pre-calculated using the pseudo-spherical photolysis scheme of PHODIS radiative transfer model and are used through a look-up table (Kylling et al., 1995).

The tropospheric concentrations of the chemical species are prescribed via model boundary conditions. The boundary conditions of water vapour and ozone are taken from the ECMWF ERA-Interim reanalysis (Dee et al., 2011) except for the water vapour boundary conditions in the sensitivity experiments which are described below. The concentration of tropospheric methane (CH_4) is from Global view-data (http://www.esrl.noaa.gov/gmd/ccgg/globalview/ch4), nitrous oxide (N_2O) concentration is from Agage data (Prinn et al., 2000), and halogens concentrations in the troposphere (Cly and Bry) are from Montzka et al. (1999) updated data. The carbon dioxide (CO_2) concentration is based on global annual mean trend data (ftp://aftp.cmdl.noaa.gov/products/trends/co2). At the upper boundary ($0.1\,\mathrm{hPa}$) climatological values of water vapour and ozone averaged over 2005–2013 from MLS data were used.

The FinROSE-CTM has been used to study the impact of meteorological conditions on water vapour trends (Thölix et al., 2016), ozone/NO_x chemistry (Salmi et al., 2011) and ozone chemical loss (Karpechko et al., 2013), and the model results showed good agreement with observations. Also future ozone losses have been investigated by using driving data from a chemistry–climate model (Damski et al., 2007a).

For this study, three simulations covering the Arctic winters between 2009/2010 and 2015/2016 were performed. The simulations differed from each other by the prescribed water vapour concentration in the tropical tropopause region (stratosphere

between 21° S–21° N, below 80 hPa), where it was prescribed as follows: (1) water vapour from ERA-Interim (Interim), (2) 1.6× Interim (Max), (3) 0.5× Interim (Min). The SWV lower boundary conditions for Min and Max simulations were obtained by scaling the reanalysis data in the tropical tropopause layer (TTL), around 80 hPa, between 21° S-21° N, so that they approximately correspond to the driest and wettest CCMVal-2 models, as determined by SWV values at the tropical tropopause

5   (Gettleman et al., 2010). This construction allows us to isolate the influence of the tropical water vapour on stratospheric chemistry while keeping all other factors fixed, and thus to estimate the contribution of processes controlling tropical water vapour entry values to Arctic ozone loss. Eight simulated years before 2009 are considered spinup and were not analysed. Ozone was initialised with ERA-Interim ozone in every year, in the beginning of December. The water vapour was not adjusted and allowed to evolve freely through the whole period of integrations. Ozone and water vapour observations from the Microwave

10   Limb Sounder (MLS) abroad Aura satellite (Lambert et al., 2007) were used to validate the reference simulation. MLS data is shown as 5 day averages because of the small amount of data covering the polar vortex in some cases.

3   Results

Model simulations were made for seven winters (2009–2016), but only four of them are discussed here. The four selected Arctic winters, 2010/11, 2012/13, 2013/14 and 2015/16 differ from each other with respect to the stratospheric temperatures

15   and polar vortex strength. They provide examples of different role of SWV in ozone loss in mild (2012/13) cold (2010/11, 2015/16) and intermediate (2013/14) stratospheric winter conditions.

3.1   Temperature and water vapour

The boundary condition at the tropical tropopause for the reference simulation was evaluated by comparing simulated water vapour concentrations with observed ones from MLS. The top panels in Fig. 1 show daily mean water vapour at 80 hPa

20   averaged between 21° S and 21° N for two representative years 2013 and 2014. The temperature for the same region is shown in the lower panels. The cold point, where SWV boundary conditions were prescribed, is just below the 80 hPa level. The temperature shows the typical annual cycle in the TTL with minimum in northern hemisphere (NH) winter and maximum in NH summer. The temperature in the TTL controls how much water vapour enters the stratosphere by freeze drying the upwelling air (e.g., Fueglistaler et al., 2005). As a result the maximum water vapour concentration occur in the NH autumn

25   and minimum in early NH spring. The effect of interannual variability and shorter term variations in the temperature on stratospheric water vapour can also be seen, e.g. the low temperature in early 2013 results in 0.5–1 ppm less water vapour than during the same time in 2014.

The Interim simulation produces water vapour concentrations comparable to the amount seen by MLS (Fig. 1), which shows that the boundary condition is reasonable. However, Interim variability leads that of MLS by 3–4 weeks suggesting that the

30   Brewer–Dobson circulation in ERA-Interim responsible for upward transport of the water vapour anomalies in the tropics could be too fast (Simmons et al., 1999; Schoeberl et al., 2012; Monge-Sanz et al., 2013). The Max simulation has 2–3 ppm more water vapour in the tropics than the Interim simulation, while the Min simulation is about 1.5 ppm drier than the Interim

simulation. A closer look at the SWV differences between the simulations in the tropics suggests that while the Max/Interim ratio is between 1.55 and 1.6, i.e. very close to 1.6 and in line with the prescribed boundary condition, the Min/Interim is about 0.55–0.6 suggesting that the Min run gains a small amount of water while transporting air upward.

We next describe the meteorological condition in the Arctic stratosphere during the analysed winters. Figure 2 shows the daily average temperature in the Arctic polar vortex in winters 2010/11, 2012/13, 2013/14 and 2015/16. The polar vortex was identified using the modified potential vorticity (mPV) (Lait, 1994). Here the polar vortex is defined as the area enclosed by the 36 PVU isoline. The winter 2010/11 represents a cold winter with vortex average temperatures below 200 K and minimum temperatures below 195 K, sufficient for formation of NAT/STS PSCs, through most of the winter, from December to the beginning of April with only a brief interruption by a warming in early January. Minimum temperatures in the vortex were record cold and below 190 K even in the end of March (Manney et al., 2011). The winter 2012/13 is an example of a warm Arctic stratospheric winter. Vortex average temperatures below 195 K were seen for only a few days in December in the ERA-Interim data, and the minimum temperature was below 195 K until mid January. A SSW occurred in early January followed by a weakening and a break up of the polar vortex in the lower stratosphere already in February. The winter 2013/14 was intermediate with average temperatures inside polar vortex being close to long-term climatological mean through most of the winter, until late March when a final SSW occurred. There were only a few days in late December when the average temperature was below 195 K. The 2015/16 winter was as cold, or even colder, as the 2010/11 winter during December–February with minimum vortex average temperatures below 195 K. However, a minor SSW occurred in early February and the final warming came in early March, ending the cold period and reducing ozone depletion potential much earlier than in the 2010/11 winter.

Figure 3 shows the five day running mean concentration of water vapour at 54 hPa averaged over the Arctic polar vortex for winters 2010/11, 2012/13, 2013/14 and 2015/16. The gaps in the 2012/13 MLS curve are due to undefined vortex (or a too small vortex with only few observations) after the SSW. The water vapour concentration in the Interim simulation is comparable to the MLS data. However, the variability in water vapour is smaller in FinROSE than in the MLS data. Typically there is a stronger increase in the water vapour towards the spring in MLS than in the simulation. This is most evident in winter 2013/14 when MLS concentrations increased by more than 1 ppm between November and April while the simulated increase was only 0.3 ppm. Although an increase by spring is expected due to downward transport of air with higher SWV concentration by the BD circulation the increase seen in MLS observations in 2014 is unusual. For example the observed increase in January 2013 after the SSW associated with downward transport of water-rich air from above was about 0.3 ppm and that increase was reasonably well reproduced by FinROSE. Note that the MLS observations within the polar vortex are sparse, which adds some noise to the MLS vortex average. Also note that FinROSE vortex-mean values are calculated using all data points inside the vortex even if MLS data are not available for each point. This approach increases the robustness of model estimates but at the same time complicates direct comparison with MLS. Interestingly, when looking at the 60–90° N average, which includes also air from outside the polar vortex, there is no similar spring increase in MLS data as seen in (Fig. 3), and the agreement between FinROSE and MLS improves (not shown). In all winters, the Max simulation has about 2 ppm more water vapour in the Arctic polar vortex than the Interim simulation, and the Min simulation is about 1.5 ppm drier than the Interim

simulation. This indicates that the simulated differences in the polar vortex water vapour are about the same as the differences in the boundary conditions for the tropical tropopause (Fig. 1), despite the average increase in SSW between the TTL and the polar vortex of about 1.5 ppm in each run.

There are also several SWV decreases seen in Fig. 3 which are due to the formation of ICE PSCs and possibly also to dehydration due to sedimentation of ICE particles. The most pronounced one is in the winter 2015/16 when, during a very cold period (Fig. 2), the observed concentrations decreased from 5.2 ppm to 4.7 ppm and remained low until late February. A relatively small decrease of only about 0.2 ppm was simulated in the Interim run. This decrease corresponded to formation of ICE PSCs in the model (see Section 3.2 for discussion of PSC results) and therefore at least a part of the decrease could be explained by sedimentation. A much larger decrease of about 1 ppm was seen in the Max simulation starting from late December, which is consistent with larger amounts of ICE PSCs simulated in this run. Another, much smaller, decrease of about 0.2 ppm can be seen in the MLS observations during mid-January 2011 corresponding to a cold period. The decrease is almost undistinguishable in the Interim simulation, but is pronounced in the Max simulation, which is a result of a larger amount of ICE PSCs.

3.2 Polar stratospheric clouds

Table 1. Sum of the ICE and NAT/STS PSC volumes (10^6km^3*day).

	Year	2010/11	2012/13	2013/14	2015/16
ICE	Interim	94	17	27	499
	Min	5	0	0	105
	Max	425	160	183	1150
NAT/STS	Interim	19487	9642	20417	22128
	Min	17751	8600	18220	20939
	Max	19919	10007	21474	22034

Figure 4 and 5 show PSC type 2 (ICE) and PSC type 1 a and b (NAT/STS) volumes between 15 and 37 km (about 375 and 950 K) in the Arctic polar vortex for winters 2010/11, 2012/13, 2013/14 and 2015/16. The volume was calculated by summing the volumes of model grid boxes containing PSCs. NAT/STS PSC is assumed to exist in the gridbox if there is liquid HNO_3 more than 0.3 ppt. In the winter 2010/11 the polar vortex was stable and cold, but not extremely cold. The ICE PSC volume (Fig. 4) in the Interim simulation was mostly moderate except for a period in late January with cold temperatures and large ICE PSC volumes. The ICE PSCs lasted longer in the spring than in other winters. It is unusual that ICE PSC:s occur after January, but in 2011 ICE PSCs were seen through February even in the Interim simulation. In the Max simulation the ICE PSCs lasted until mid March. Also the Cloud-Aerosol Lidar and Infrared Path finder Satellite Observation (CALIPSO) (Pitts et al., 2007) observed PSCs in the 2010/11 winter. The observed ICE PSC areas are comparable to the FinROSE modelled

ICE areas (Thölix et al., 2016). Also the duration of ICE clouds is comparable. In the winter 2012/13 the polar vortex was very cold in December, and some ICE PSCs were simulated. However, after the SSW in early January no ICE PSCs were simulated, not even in the Max simulation. The 2013/14 winter was moderately cold with some ICE PSC occurrence in late January. For example too dry models may not be able to simulate a large Arctic ozone loss such as of 2010/11. The winter
5 2015/16 started as very cold in December and January, and the ICE PSC volume was large through January. The maximum ICE PSC volumes in the Interim simulation were more than 50 % larger compared to the other cold winter 2010/11. Dörnbrack et al. (2017) and Khosrawi et al. (2017) also reported unprecedented and widespread ICE PSC formation seen in CALIPSO observations in 2015/16. This was also the only winter with a significant ICE PSC volume in the Min simulation, with a water vapour concentration of only about 3.7 ppm.
10 The water vapour concentration had a strong effect on the ICE PSC formation: in the Max simulations the ICE PSC volume increases significantly in all winters. For instance in 2010/11 the largest PSC volume is more than twice as large in Max as in the Interim simulation. In the warm winters (2012/13 and 2013/14) the relative increase in the ICE PSC volume due to additional water vapour was even larger than in the cold winters (2010/11 and 2015/16). The amount of water vapour was an important factor for the extent of ICE PSC occurrence also in winter 2015/16, however, the relative increase between the
15 Interim and Max simulation was smaller than in other studied winters, that were warmer. PSC starts to form about two weeks earlier in the Max simulation compared to the Interim simulation. In the Min simulation the stratosphere is too dry for ICE PSC formation in nearly all years.

Figure 5 shows the volume of NAT/STS PSCs in the Arctic vortex. NAT/STS volumes are always significantly larger than the ICE volumes because type 1 PSCs form at warmer temperatures than ICE PSCs. Type 1 PSCs typically start to form in
20 early November and ICE PSCs in mid to late December. The simulated peak values in the NAT/STS volume range from 260 to 340 million km^3, while the ICE volume peaks range from 4 to 30 million km^3 in the Interim simulation. As expected the type 1 PSCs occur later in the spring than ICE PSCs, e.g. in the winter 2010/11 NAT/STS PSCs were simulated until late April, more than a month later than the ICE PSCs.

In the cold winter 2010/11 NAT/STS PSCs persisted for almost five months, from December to April. An increase in
25 moisture (Max simulation) had only a minor effect on the NAT/STS volume. In the Min simulation the maximum NAT/STS volume was usually about 20 million km^3 smaller than in Interim simulation, while the difference between Max and Interim was much smaller. In the 2012/13 winter NAT/STS PSCs were simulated only in the beginning of the winter and by early January all the PSCs disappeared due to warm conditions. The maximum values of NAT/STS volumes in 2012/13 winter were large, 330 million km^3, and the difference between Interim and Min simulation is more than 30 million km^3. The increase of
30 water vapour in the Max simulation did not change the PSC volume much. In the early 2013/14 winter the NAT/STS volume was even larger than in 2010/11, but warmer temperatures in the vortex in February caused the PSC volume to diminish more rapidly. The effect of water vapour was the largest among the simulated years, the increase in NAT/STS volume between Min and Interim simulations was 30–40 million km^3. The NAT/STS volumes in the 2015/16 winter were larger than in 2010/11, but the PSCs did not persist as late as in 2010/11. The increase in type 1 PSC volume due to increased water vapour was smaller
35 than in 2013/14, about 25 million km^3.

Table 1 shows cumulative ICE and NAT/STS PSC volumes between the altitudes 15 and 37 km. The largest cumulative ICE volumes are always seen in the Max simulations. In the Min simulations there are only very small or no ICE PSC volumes, with the exception of the winter 2015/16, when considerable ICE PSC volume was present in all runs. However, in 2015/16 the ICE PSCs occurred mainly in December and January, while in 2010/11 the ICE PSCs occurred from January until the end

5 of February. The timing of the PSCs is important for chlorine activation and ozone loss as discussed later. The effect of water vapour on the cumulative ICE PSC volume is larger in warm years than in cold years. The NAT/STS volume also strongly depends on winter temperatures – the maximum volume is simulated in the coldest winter 2015/16 in every simulation, while the smallest volume is simulated during the warmest winter 2012/13. However, unlike ICE PSC, the NAT/STS clouds are formed in every winter. The formation of type 1 PSCs is less sensitive to changes in water vapour concentration than the ICE

10 PSCs. The relatively large changes in water vapour between different simulations results in relatively small small changes in the cumulative NAT/STS volume.

3.3 Chlorine activation

Table 2. Vortex-mean mixing ratio integrated over the winter of activated chlorine in Arctic vortex in different runs (ppb*day). Percentage in parentheses indicate the effect of SWV concentration change compared to Interim simulation.

Year	2010/11	2012/13	2013/14	2015/16
Interim	148	69	110	115
Min	141 (-5 %)	68 (-1 %)	97 (-12 %)	113 (-2 %)
Max	157 (+6 %)	72 (+4 %)	116 (+5 %)	119 (+3 %)

In early winter chlorine is present as reservoir compounds (HCl and $ClONO_2$), which do not destroy ozone. When PSCs start to form in the cold conditions within the polar vortex the chlorine species are transformed into intermediate species such

15 as Cl_2. These species are easily dissociated when the sunlight reaches the polar vortex in the spring to form active chlorine species that participate in the catalytic ozone depletion cycles, i.e. ClO_x (ClO, Cl_2O_2 and Cl). PSCs sustain the regeneration of ClO_x.

Figure 6 shows the fraction of reservoir, intermediate and active chlorine species at 54 hPa in the Min and Max simulations. The results from the Max simulation are represented by the upper limit for the intermediate (magenta) and active species

20 (green), and by the lower limit for the reservoir species (black). The chlorine fractions from the Interim simulation always fit within the range from the Min and Max simulations. The timing of the changes in the partitioning of the chlorine species correlates well with the occurrence of PSCs, both NAT/STS and ICE. NAT/STS PSC volume starts to grow at the same time when chlorine starts to transform from reservoirs to intermediate species (Fig. 5).

In the 2010/11 winter chlorine activation starts in the latter half of December and the fraction of ClO_x is large through the

25 January–Mach period, reaching the maximum of about 85 %. The active chlorine starts to transform back to reservoirs in the beginning of March. In early April when the PSCs disappear the active chlorine rapidly decreases to the background values.

In the 2012/13 winter chlorine activation starts slightly earlier than in the other years, but already in the beginning of February most of the chlorine has converted back to reservoir species due to a SSW. The maximum fraction of ClO_x is about 75 %, and it is reached already in the end of December. The period with active chlorine lasted only for a short period, the active chlorine decreased during January, and in the beginning of February the concentration reached nearly background values.

5   The beginning of the winter 2013/14 winter was very cold, chlorine activation started in mid December, and the maximum chlorine activation is reached already in the end of January. After that the vortex warmed and chlorine transformed back to reservoir species. The maximum fraction of ClO_x is slightly lower than in cold winters, about 70 %.

    The 2015/16 winter started similar to the cold winter 2010/11 and nearly all of the chlorine was activated at the beginning of January, but the deactivation started already in the end of January making the period with high ClO_x rather short. In the end

10   of February the vortex warmed up and chlorine transformed back to reservoir species. The maximum fraction of the activated chlorine of about 80 % was reached by the beginning of January.

    The water vapour concentration seem to strongly affect the transformation of chlorine from the reservoir species to the intermediate ones in the beginning of Arctic winter. The fractions of intermediate and reservoir chlorine species change significantly with water vapour concentration in November and December, when NAT/STS PSCs start to form. The difference between Min

15   and Max simulations can be up to 30 % when about half of the reservoir chlorine have transformed to intermediate species, just before the concentration of active chlorine species starts to increase. The concentrations of the active and reservoir chlorine species differs significantly between the Min and Max simulations during the period with high ClO_x, except for the 2016 spring. The water vapour content has less effect on the intermediate chlorine species during the chlorine activation period. In the cold spring 2011 the difference in chlorine activation between Min and Max simulations was about 5 % on average,

20   it reached nearly 20 % in the beginning of April, when the chlorine deactivation was fast. In the warm winter 2012/13 the difference was less significant, about 5 % during the whole short activation period. In 2013/14 winter the difference reached 10 % in the latter half of January. Between mid February and mid March the difference is 15–18 %. The chlorine activation in 2015/16 winter seems to be less dependent on water vapour content. The difference between simulations is only few percents, only when the deactivation starts (in the end of February) the difference is more than 5 %.

25   The effect of increased water vapour seems to be large in moderately cold years, i.e. when the chlorine activation is not so complete. The amount of chlorine activation correlate with the volume of NAT/STS PSCs. Also the end of chlorine activation depends on the existence of NAT/STS PSCs. ICE PSC volume instead does not correlate with chlorine activation. For example in 2012/13 and 2013/14 winters there were no ICE PSC in the Min simulation but the chlorine activation is nearly as high as in the Max simulation, which have ICE PSCs.

30   Table 2 shows the cumulative sum of activated chlorine within the polar vortex. The changes in water vapour between the Min/Interim/Max simulations have the largest effect on the cumulative ClO_x in moderately cold winters (2010/11 and 2013/14). The increase from Interim to Max was +5 to 6 % and change from Interim to Min was -5 to -12 %. In the cold winter 2015/16 the respective changes were +3 and -2 %, and in the warm winter 2012/13 the changes were +4 and -1 %.

3.4 Ozone loss

Figure 7 shows the mean chemical total ozone loss within the polar vortex for all the studied winters 2010/11, 2012/13, 2013/14 and 2015/16. The total column chemical ozone loss was calculated by subtracting the passive transported total ozone from the modelled total ozone. However, the polar vortex is defined here using the potential vorticity limit 36 PVU only at the 475 K

5   level. The figure shows the chemical ozone depletion in the Interim, Min and Max simulations as well as the difference in the loss between the Min and Max simulations. The passive ozone tracer was initialized every year on December 1st, when it was set equal to the ozone in the model. Chemical processes start to reduce ozone already in December, but they have minor effect on the total wintertime ozone loss. In January the chemical processes become more intensive, when the chlorine activation increases (see Fig. 6).

10   In general the ozone loss is larger in cold years. The largest ozone loss was simulated in the beginning of April 2011 when about 90 DU ozone had been destroyed according to our model. FinROSE seems to underestimate the ozone loss, possibly due to a general 10 % negative bias in total ozone, for example Sinnhuber et al. (2011) and Manney et al. (2011) simulated 120 DU ozone loss and Pommereau et al. (2013) even 170 DU in winter 2010/11. If we look at maximum ozone losses instead of the polar vortex mean losses, then the numbers are larger. The maximum ozone loss in 2010/11 within the polar vortex was

15   128 DU, which is comparable to the Sinnhuber et al. (2011) value.

The ozone loss in the warm winter 2012/13 differs from the loss in colder winters (2010/11 and 2015/16). In winters when the polar vortex is unstable and small or disturbed the Brewer–Dobson circulation brings more NO_x-rich air to the polar vortex than usual. Hence the ozone loss in the 2012/13 winter was produced mostly by NO_x chemistry as shown previously by e.g., Sagi et al. (2017). The total ozone column loss in this winter remained smaller than in cold years, when the ozone depletion is

20   driven by halogens. By the end of April 2014 the simulated vortex mean ozone loss was about 75 DU in the Interim simulation. Before mid February, i.e. during the coldest period, there was very little effect from the changes in SWV. A relatively small ozone loss of 60 DU was simulated in 2015/16, which was due to the unstable polar vortex, which split and warmed, stopping the catalytic ozone cycles and ozone loss early.

Figure 7 also shows the difference of polar vortex averaged chemical ozone loss between Min and Max simulation. It tells

25   how much the water vapour concentration change affects the ozone loss. The difference is largest (nearly 16 DU) in 2013/14, a moderately cold winter, with significant ozone depletion. Another winter, 2010/11, with significant ozone loss and cold, but not extremely cold conditions showed the second largest effect from addition of water vapour, about 10 DU. In 2012/13, when the ozone loss was mostly caused by NO_x chemistry, the difference between Min and Max simulations was about 7.5 DU. The 2015/16 winter started as very cold, but warmed early. The difference in ozone loss between the simulations remained

30   very small up to mid February, by mid March the difference was about 8 DU. A reduction in the water vapour decreased ozone loss in every winter. In the Interim simulation the deepest ozone losses were about 3–8 DU (5–10 %) deeper than in the Min-simulation. The effect from an increase in water vapour from Interim to Max was about same. In 2010/11 winter the loss increased by about 7 %, while Sinnhuber et al. (2011) and Vogel et al. (2011) reported an increase of ozone loss by 20 % and 10 % (respectively) with water vapour increase being of about the same magnitude as here. Thus, our estimates are

slightly smaller than those by Vogel et al. (2011). The reason for the difference is not clear, but FinROSE's horizontal resolution ($3° \times 6°$) may be too coarse to capture the deepest ozone loss.

The changes in the amount of water vapour is not very important for ozone loss in cold years, within the range that was tested here. In the 2010/11 winter the chlorine activation was nearly complete in the Arctic polar vortex, and additional water
5   vapour did not increase chlorine activation and thus not the ozone depletion. Increasing water vapour concentration (compared the Interim simulation) strengthen ozone loss at least 4 DU at other winters except for 2011 when the increase is not significant.

Table 3. Maximum polar vortex-mean ozone loss produced by full chemistry, heterogeneous chemistry and separately the NAT/STS and ICE part in Min, Max and Interim simulations (DU). Percentages show the fraction due to each part relative to the full chemistry.

	Year	2010/11	2012/13	2013/14	2015/16
Min	Full chemistry	84	54	75	58
	Heterogeneous part	50 (60 %)	11 (21 %)	28 (38 %)	37 (64 %)
	NAT/STS and ICE	20 (24 %)	5 (10 %)	11 (15 %)	14 (24 %)
Interim	Full chemistry	90	56	83	62
	Heterogeneous part	56 (62 %)	14 (25 %)	36 (44 %)	41 (66 %)
	NAT/STS and ICE	30 (33 %)	8 (15 %)	21 (25 %)	20 (32 %)
Max	Full chemistry	91	61	90	66
	Heterogeneous part	56 (62 %)	18 (30 %)	42 (47 %)	44 (66 %)
	NAT/STS and ICE	34 (37 %)	11 (18 %)	27 (30 %)	24 (36 %)

To better understand the mechanism of SWV influence on ozone loss, simulations without heterogeneous chemistry were performed. From those simulations ozone loss caused by heterogeneous chemistry can be separated by subtracting the total ozone simulated without heterogeneous chemistry from that simulated in the full chemistry run. Two different set-ups were used
10   for testing the effect of the heterogeneous chemistry. In the first gas-phase chemistry simulation the heterogeneous chemistry was not included at all. In the second simulation the formation of PSCs was limited by setting the air temperature passed to the heterogeneous chemistry module to 200 K, similarly to what was done in Karpechko et al. (2013). This setting has little influence on the reactions on the background aerosols, but prohibits formation of STS, NAT and ICE PSCs. Table 3 summarises ozone loss characteristics during the studied years and shows the loss produced by full chemistry, heterogeneous chemistry and
15   separately the NAT/STS and ICE PSCs in Interim, Min and Max simulations.

In the Interim simulation with full chemistry in 2010/11 about 90 DU ozone was depleted, of which the heterogeneous chemistry caused 56 DU depletion, i.e. about 62 % of the total ozone loss. Heterogeneous chemistry due to ICE and NAT/STS PSCs destroyed 30 DU ozone, which was about 33 % of the total loss. The increase of water vapour (Max simulation) did not increase the ozone loss, but in the Min simulation there was 6 DU less ozone depletion. This is consistent with the results by
20   Kirner et al. (2015), who argue that the contribution of ICE PSCs to the ozone loss is always less than 5% in the Antarctic spring, where the chlorine activation is nearly complete.

In the warm 2012/13 winter the heterogeneous part is only 25 %. NAT/STS and ICE PSCs caused only a very small part of the total heterogeneous chemistry driven ozone loss. The loss caused by heterogeneous chemistry increased with increasing water vapour, but remained small even in the Max simulation.

In 2013/14 the heterogeneous chemistry destroyed about 36 DU (44 %) of the ozone and ICE and NAT/STS about 21 DU (25 %), when the total ozone loss was 83 DU in the Interim run. The increase in SWV from Interim to Max increased the ozone loss by about 7 DU and the decrease in SWV from Min to Interim decreased the ozone loss by 8 DU. So, water vapour changes have larger role than in colder year. The ozone depletion due to heterogeneous chemistry increased with water vapour, even though the fraction due to heterogeneous chemistry was smaller than in 2010/11 and 2015/16.

In the 2015/16 winter the heterogeneous part was largest when compared to other simulated years, reaching even 66 % of the ozone loss, and also the ICE and NAT/STS part was large, 32 %. The total ozone loss is however only 62 DU about the same as in 2012/13 winter. When the water vapour content was increased from Interim to Max simulation, the fraction due to the heterogeneous chemistry remained the same, but the fraction due to NAT/STS and ICE PSCs increased.

Based on the results in Table 3 it can be concluded that nearly all SWV impact on ozone loss is through heterogeneous chemistry. For example in 2010/11 the ozone loss without heterogeneous chemistry was 34 DU in Interim, 34 DU in Min and 35 DU in Max simulation and only the heterogeneous part changed from model run to model run. In 2012/13 and 2013/14 the non-heterogeneous contribution is 42 and 47 DU respectively, and in 2015/16 21 DU, i.e. in warm years it is larger than in cold years.

Finally we analyse the vertical distribution of the ozone loss and the effect of SWV on ozone loss, which is shown in Fig. 8. The largest ozone loss was simulated in 2010/11, when the ozone destruction in the Interim run with normal SWV was about 1.4 ppm between 60–30 hPa. The ozone depletion increased by 0.2 ppm between the Min and Max simulations. In 2012/13 the maximum ozone reduction is almost the same as in 2010/11, but it occurs at higher altitude (NO_x induced) and lasts for shorter period than in 2011. The effect of the increase in water vapour from Min to Max simulation had only a minor effect on the ozone depletion in 2012/13. The heterogeneous chemistry and chlorine activation did not have an important role in the warm conditions. In the 2014 spring the conditions in the polar vortex remained favourable, but the temperature was not as low as in 2011. The ozone loss developed steadily, but remained moderate. The two winters 2010/11 and 2013/14 with the most favourable conditions for halogen driven ozone depletion showed the largest increase in ozone loss with water vapour. The effect was more clear in 2013/14, which was the warmer of the two winters. The winters 2010/11 and 2015/16 look similar during January–February, but the ozone loss became much more severe in 2010/11 due to favourable conditions in March–April. In 2015/16 there was a very cold period, but it occurred too early to have a large impact on the ozone depletion, and therefore the water vapour increase had only a moderate effect later in the spring. In 2013/14 the largest ozone loss is about 1.2 ppm between 60 and 30 hPa while in 2015/16 it is only about 1 ppm at the same altitude. Livesey et al. (2015) and Sagi et al. (2017) showed results from 450 K level, and their ozone losses were about 2 ppm in winter 2011. In winter 2013 Sagi et al. (2017) had about 1.5 ppm ozone loss, which is about the same as we found.

4   Discussion and conclusions

Warmer climate in the troposphere in the future leads to increasing water vapour concentrations in the stratosphere (Dessler et al., 2013), which further warms the climate due to water vapour feedback. Khosrawi et al. (2016) showed that an increase in SWV and a cooling of the stratospheric temperature enhances each other, the volume of PSCs increases and they last longer in the vortex. The ozone loss can thus increase although the halogen loading has been decreased. In this study, rather than artificially changing the temperature we used meteorological fields from seven winters during the period 2010–2016 with different temperatures and dynamical conditions in the stratosphere. We changed the water vapour content in the tropical tropopause region according to the CCMVal-2 simulations. The water vapour entry concentration is controlled by the cold point in the TTL, and the distribution of SWV is largely determined by this entry concentration together with the transport and the contribution from methane oxidation. Results show that, as expected, wetter/drier tropical tropopause leads to wetter/drier Arctic polar vortex and also the size of polar ozone depletion changes along the water vapour changes. For example too dry models may not be able to simulate a large Arctic ozone loss such as of 2010/11, which can be seen from the Table 3.

A reduction in SWV decreases the ozone loss due to heterogeneous processes by decreasing the PSC formation. An increase in SWV instead makes the heterogeneous chemistry more important by increasing PSCs. If the winter is cold enough, the increase is less important, because the PSC volume is large anyway, and the chlorine activation is already nearly complete in Arctic vortex. As expected, heterogeneous chemistry is more important if the winter is cold and PSC volumes are large. In winters 2010/11 and 2015/16 over 62 % of the ozone loss is initiated by heterogeneous chemistry, and in the warm winter 2012/13 about 21 %. In winter 2010/11 Pommereau et al. (2013) got 120 DU ozone loss due to heterogeneous reactions, which is about 70 % of the total loss.

Winters in the stratosphere are often divided into cold, or dynamically inactive, and warm, or dynamically active. In the cold winters the polar vortex is stable and more PSCs are formed and halogens can destroy ozone. Warm conditions in the winter stratosphere are often due to SSW, which allows NO_x-rich air masses from the mesosphere to enter the vortex and take part in the ozone depletion (Sagi et al., 2017). Cold winters differ from the warm winters when looking the ozone loss and the fraction of ozone loss initiated by heterogeneous chemistry. Also the PSC volumes and thus chlorine activation are in higher level during cold winters. A lack of water leads to less ICE PSCs, and therefore to less ClO_x. However, the ICE PSC volume is not the only explaining factor for ozone loss. The type 1 PSCs that form at higher temperatures are responsible for a large fraction of the chlorine activation. The formation of STS and NAT is limited by the partial pressure of nitric acid, sulfuric acid and water and hence the concentration of water vapour is not the only thing affecting the NAT/STS volume. However, the dry conditions in the Min simulations have some limiting effect on the peak NAT/STS volume.

The cold winter 2010/11 differs from the others by an especially long chlorine activation period, which lead to large ozone depletion. In the warm winter 2012/13 the polar vortex was weak; however it was shifted to south where it was exposed to sun-light earlier than usually, and thus ozone loss could start earlier. The ozone loss was however weak because chlorine activation remained very low. The ozone depletion in 2012/13 occurred at higher altitudes than in the other years, because of the NO_x induced ozone loss. The 2013/14 winter was moderately cold, and the ozone depletion was second largest among

the considered winters. In this winter the effect of water vapour changes on ozone loss was the largest across the studied winters. Winter 2015/16 started as extreme cold (Matthias et al., 2016; Manney et al., 2016), but the stratosphere warmed early terminating chlorine activation and leaving ozone loss relatively low, despite the fact that the cumulative ICE (and NAT/STS) volumes were extremely large.

5   Chemical ozone destruction inside the Arctic vortex varied between 56 and 90 DU in the Interim-simulations, 61 and 91 DU in the Max-simulations and 54 and 84 DU in the Min simulations. We find that the meteorological conditions are more important for the ozone depletion than the concentration of water vapour. Also the fraction of heterogeneous chemistry in the ozone loss is more dependent on the temperature than on the water content. Livesey et al. (2015) arrived to similar conclusion, when investigating ozone loss based on the MLS observations.

10   MacKenzie and Harwood (2004) showed from their chemistry–climate model simulations, that the increase of water vapour increases the volume of PSCs both by microphysical effects and due to lowering the stratospheric temperatures. The microphysical processes cover about 20 % of the increase and the rest is due to cooling of the stratosphere. In our study the volume of ICE PSCs increased by 20 %, but only due to the microphysics. The increase could have been larger with temperature changes in the simulations. However, the temperature effect can be seen by investigating different years. The difference in cumulative

15   ICE volumes between studied years was as large as factor 20, and in cumulative NAT/STS volumes it varied by factor 2. MacKenzie and Harwood (2004) got about 15 % more ozone loss at 465 K level with less than 1 ppm additional water vapour without changing temperature. In our study the ozone loss increased by 1 DU (1 %) in 2010/2011, 5 DU (9 %) in 2012/2013, 7 DU (8 %) in 2013/2014 and 4 DU (6.5 %) in 2015/2016 when the water vapour concentration was increased by about 2 ppm. When the water vapour was instead decreased by about 1.5 ppm, the ozone loss decreased by 6 DU (6.7 %), 2 DU (3.6 %),

20   8 DU (10 %) and 4 DU (6.5 %), respectively. The small contribution due to water vapour increase in winter 2010/11 can be compared to the results of MacKenzie and Harwood (2004) in the Antarctic vortex. There the chlorine activation is nearly complete in every winter. In winter 2010/11 also in Arctic vortex the chlorine activation was nearly complete, and additional water vapour did not change the activation and, thus not either the ozone depletion.

Note that effects of changing water vapour concentration on air temperature, not accounted for here, would probably have

25   increased the water vapour impact on ozone loss. The indirect impact comes through water vapour radiative impact on stratospheric temperatures. Tian et al. (2016) estimates that a 2 ppm increase of water vapour would cool the stratosphere by approximately 2 K, while Rex et al. (2004) estimates that a 1 K cooling could increase ozone loss in the Arctic by 15 DU. Thus based on these estimates a water vapour increase of 2 ppm, similar to the difference between Interim and Max runs, could result in up to 30 DU additional ozone loss. This estimate suggest that the direct water vapour impact on ozone loss quantified in our

30   experiments may account for only about 20 % of total ozone loss, but in order to confirm this estimation a designed experiment with a chemistry–climate model would be needed.

In summary, we find that variability of stratospheric water vapour of 3.5 ppm, comparable in magnitude to uncertainty in simulated water vapour concentration near the tropical tropopause, results in differences in simulated Arctic ozone loss up to 15 DU, i.e. more than 10 % of the total chemical ozone loss in the Arctic vortex. Better understanding of tropical processes

contributing to the stratospheric water vapour concentration, and thus constraining stratospheric water vapour, would therefore reduce the uncertainty in Arctic ozone loss and improve future projections of ozone layer recovery.

Competing interests. The authors declare that they have no conflict of interest.

Data availability. Data from the FinROSE simulations is available from the authors upon request. MLS data is available at https://mls.jpl.nasa.gov.

5   *Acknowledgements.* We acknowledge ECMWF for providing us the ERA-Interim reanalysis data. We also want to thank the UARS reference atmosphere project and MLS/Aura teams for water vapour data. The MLS data were obtained through the Aura MLS website (http://mirador. gsfc.nasa.gov/). Funding by the Academy of Finland through the UTLS project (140408) and by the EU through the project GAIA-CLIM is gratefully acknowledged.

References

Atkinson, R., Baulch, D. L., Cox, R. A., Crowley, J. N., Hampson, R. F., Hynes, R. G., Jenkin, M. E., Rossi, M. J., and Troe, J.: Evaluated kinetic and photochemical data for atmospheric chemistry: Volume III – gas phase reactions of inorganic halogens, Atmos. Chem. Phys., 7, 981–1191, doi:10.5194/acp-7-981-2007, 2007.

Bekki, S. and Pyle, J.: Two-dimensional assessment of the impact of aircraft sulphur emissions on the stratospheric sulphate aerosol layer, J. Geophys. Res., 9, 15839–15847, 1992.

Chipperfield, M. P., Dhomse, S. S., Feng, W., McKenzie, R. L., Velders, G. J. M., and Pyle, J. A.: Quantifying the ozone and ultraviolet benefits already achieved by the Montreal Protocol, Nat. Commun., 6, 7233, doi:10.1038/ncomms8233, 2015.

Dameris, M., and Godin-Beekmann, S. (Lead Authors), Alexander, S., Braesicke, P., Chipperfield, M., de Laat, A.T.J., Orsolini, Y., Rex, M., and Santee, M.L.: Update on Polar ozone: Past, present, and future, Chapter 3 in Scientific Assessment of Ozone Depletion: 2014, Global Ozone Research and Monitoring Project – Report No. 55, World Meteorological Organization, Geneva, Switz erland, 2014.

Damski, J., Thölix, L., Backman, L., Taalas, P., and Kulmala, M.: FinROSE – middle atmospheric chemistry and transport model, Boreal Environ. Res., 12, 535–550, 2007b.

Damski, J., Thölix, L., Backman, L., Kaurola, J., Taalas, P., Austin, J., Butchart, N., Kulmala, M.: A chemistry-transport model simulation of middle atmospheric ozone from 1980 to 2019 using coupled chemistry GCM winds and temperatures, Atmos. Chem. Phys., 7, 2165–2181, 2007a.

Dee, D. P., Uppala, S. M., Simmons, A. J., Berrisford, P., Poli, P., Kobayashi, S., Andrae, U., Balmaseda, M. A., Balsamo, G., Bauer, P., Bechtold, P., Beljaars, A. C. M., van de Berg, L., Bidlot, J., Bormann, N., Delsol, C., Dragani, R., Fuentes, M., Geer, A. J., Haimberger, L., Healy, S. B., Hersbach, H., Holm, E. V., Isaksen, L., Kallberg, P., Kohler, M., Matricardi, M., McNally, A. P., Monge-Sanz, B. M., Morcrette, J.-J., Park, B.-K., Peubey, C., de Rosnay, P., Tavolato, C., Thepaut, J.-N., and Vitart, F.: The ERA-Interim reanalysis: configuration and performance of the data assimilation system, Q. J. Roy. Meteorol. Soc., 137, 553–597, 2011.

Dessler, A. E., Schoeberl, M. R., Wang, T., Davis, S. M., and Rosenlof, K. H.: Stratospheric water vapor feedback, P. Natl. Acad. Sci. USA, 110, 18087–18091, doi:10.1073/pnas.1310344110, 2013.

Dvortsov, V. L., and S. Solomon: Response of the stratospheric temperatures and ozone to past and future increases in stratospheric humidity, J. Geophys. Res., 106, 7505–7514, 2001.

Dörnbrack, A., Gisinger, S., Pitts, M. C., Poole, L. R., and Maturilli, M.: Multilevel cloud structures over Svalbard, Mon. Weather. Rev., 145, 1149–1159, https://doi.org/10.1175/mwr-d-16-0214.1, 2017.

Eyring, V., et al.: Multimodel projections of stratospheric ozone in the 21st century, J. Geophys. Res., 112, D16303, doi:10.1029/2006JD008332, 2007.

Eyring, V., Cionni, I., Bodeker, G. E., Charlton-Perez, A. J., Kinnison, D. E., Scinocca, J. F., Waugh, D. W., Akiyoshi, H., Bekki, S., Chipperfield, M. P., Dameris, M., Dhomse, S., Frith, S. M., Garny, H., Gettelman, A., Kubin, A., Langematz, U., Mancini, E., Marchand, M., Nakamura, T., Oman, L. D., Pawson, S., Pitari, G., Plummer, D. A., Rozanov, E., Shepherd, T. G., Shibata, K., Tian, W., Braesicke, P., Hardiman, S. C., Lamarque, J. F., Morgenstern, O., Pyle, J. A., Smale, D., and Yamashita, Y.: Multi-model assessment of stratospheric ozone return dates and ozone recovery in CCMVal-2 models, Atmos. Chem. Phys., 10, 9451-9472, https://doi.org/10.5194/acp-10-9451-2010, 2010.

Feck, T., J.-U. Grooß, and M. Riese: Sensitivity of Arctic ozone loss to stratospheric H_2O, Geophys. Res. Lett., 35, L01803, doi:10.1029/2007GL031334, 2008.

Fueglistaler, S. and Haynes, P. H.: Control of interannual and longer-term variability of stratospheric water vapor, J. Geophys. Res., 110, 1–14, doi:10.1029/2005JD006019, 2005.

Gettelman, A., Hegglin, M. I., Son, S. W., Kim, J., Fujiwara, M., Birner, T., Kremser, S., Rex, M., Añel, J. A., Akiyoshi, H., Austin, J., Bekki, S., Braesike, P., Brühl, C., Butchart, N., Chipperfield, M., Dameris, M., Dhomse, S., Garny, H., Hardiman, S. C., Jöckel, P., Kinnison, D. E., Lamarque, J. F., Mancini, E., Marchand, M., Michou, M., Morgenstern, O., Pawson, S., Pitari, G., Plummer, D., Pyle, J. A., Rozanov, E., Scinocca, J., Shepherd, T. G., Shibata, K., Smale, D., Teyssèdre, H., and Tian, W.: Multimodel assessment of the upper troposphere and lower stratosphere: Tropics and global trends, J. Geophys. Res., 115, D00M08, doi:10.1029/2009JD013638, 2010.

Karpechko, A.Yu., Backman, L., Thölix, L., Ialongo, I., Andersson, M., Fioletov, V., Heikkilä, A., Johnsen, B., Koskela, T., Kyrölä, E., Lakkala, K., Myhre, C. L., Rex, M., Sofieva, V.F., Tamminen, J. and Wohltmann, I.: The link between springtime total ozone and summer UV radiation in Northern Hemisphere extratropics, J. Geophys. Res., 118, 8649–8661, doi:10.1002/jgrd.50601, 2013.

Khosrawi, F., Urban, J., Lossow, S., Stiller, G., Weigel, K., Braesicke, P., Pitts, M. C., Rozanov, A., Burrows, J. P., and Murtagh, D.: Sensitivity of polar stratospheric cloud formation to changes in water vapour and temperature, Atmos. Chem. Phys., 16, 101–121, doi:10.5194/acp-16-101-2016, 2016.

Khosrawi, F., Kirner, O., Sinnhuber, B.-M., Johansson, S., Höpfner, M., Santee, M. L., Froidevaux, L., Ungermann, J., Ruhnke, R., Woiwode, W., Oelhaf, H., and Braesicke, P.: Denitrification, dehydration and ozone loss during the 2015/2016 Arctic winter, Atmos. Chem. Phys., 17, 12893–12910, https://doi.org/10.5194/acp-17-12893-2017, 2017.

Kirk-Davidoff, D. B., Anderson, J. G., Hintsa, E. J., and Keith, D. W.: The effect of climate change on ozone depletion through changes in stratospheric water vapour, Nature, 402, 399–401, 1999.

Kirner, O., Müller, R., Ruhnke, R., and Fischer, H.: Contribution of liquid, NAT and ice particles to chlorine activation and ozone depletion in Antarctic winter and spring, Atmos. Chem. Phys., 15, 2019–2030, doi:10.5194/acp-15-2019-2015, 2015.

Kylling, A., Stamnes, K., and Tsay, S.-C.: A reliable and efficient two-stream algorithm for radiative transfer; Documentation of accuracy in realistic layered media, J. Atmos. Chem., 21, 115-150, 1995.

Lait, L. R.: An alternative form for potential vorticity, J. Atmos. Sci., 51, 1754–1759, doi:10.1175/1520-0469(1994)051, 1994.

Lambert, A., Read, W. G., Livesey, N. J., Santee, M. L., Manney, G. L., Froidevaux, L., Wu, D. L., Schwartz, M. J., Pumphrey, H. C., Jimenez, C., Nedoluha, G. E., Cofield, R. E., Cuddy, D. T., Daffer, W. H., Drouin, B. J., Fuller, R. A., Jarnot, R. F., Knosp, B. W., Pickett, H. M., Perun, V. S., Snyder, W. V., Stek, P. C., Thurstans, R. P., Wagner, P. A., Waters, J. W., Jucks, K. W., Toon, G. C., Stachnik, R. A., Bernath, P. F., Boone, C. D., Walker, K. A., Urban, J., Murtagh, D., Elkins, J. W., and Atlas, E.: Validation of the Aura Microwave Limb Sounder middle atmosphere water vapor and nitrous oxide measurements, J. Geophys. Res., 112, D24S36, doi:10.1029/2007JD008724, 2007.

Lin, S.-J. and Rood, R. B.: Multidimensional flux-form semi-lagrangian transport schemes, Mon. Weather Rev., 124, 2046–2070, 1996.

Livesey, N. J., Santee, M. L., and Manney, G. L.: A Match-based approach to the estimation of polar stratospheric ozone loss using Aura Microwave Limb Sounder observations, Atmos. Chem. Phys., 15, 9945–9963, doi:10.5194/acp-15-9945-2015, 2015.

MacKenzie, I. A., and Harwood, R. S.: Middle-atmospheric response to a future increase in humidity arising from increased methane abundance, J. Geophys. Res., 109, D02107, doi:10.1029/2003JD003590, 2004.

Manney, G. L., Santee, M. L., Rex, M., Livesey, N. L., Pitts, M. C., Veefkind, P., Nash, E. R., Woltmann, I., Lehmann, R., Froidevaux, L., Poole, L. R., Schoeberl, M. R., Haffner, D. P., Davies, J., Dorokhov, V., Gernandt, H., Johnson, B., Kivi, R., Kyrö, E., Larsen, N., Levelt, P. F., Makshtas, A., McElroy, C. T., Nakajima, H., Concepcion Parrondo, M., Tarasick, D. W., von der Gathen, P., Walker, K. A., and Zinoviev, N. S.: Unprecedented Arctic ozone loss in 2011, Nature, 478, 469–475, doi:, 2011.

Manney, G. L. and Lawrence, Z. D.: The major stratospheric final warming in 2016: dispersal of vortex air and termination of Arctic chemical ozone loss, Atmos. Chem. Phys., 16, 15371–15396, https://doi.org/10.5194/acp-16-15371-2016, 2016.

Matthias, V., Dörnbrack, A., and Stober, G.: The extraordinarily strong and cold polar vortex in the early northern winter 2015/2016. Geophys. Res. Lett., 43, 12287–12294, doi:10.1002/2016GL071676, 2016.

5 Monge-Sanz, B. M., Chipperfield, M. P., Untch, A., Morcrette, J.-J., Rap, A., and Simmons, A. J.: On the uses of a new linear scheme for stratospheric methane in global models: water source, transport tracer and radiative forcing, Atmos. Chem. Phys., 13, 9641–9660, doi:10.5194/acp-13-9641-2013, 2013.

Montzka, S. A., Butler, J. H., Elkins, J. W., Thompson, T. M., Clarke, A. D., and Lock, L. T.: Present and future trends in the atmospheric burden of ozone-depleting halogens, Nature, 398, 690–694, 1999.

10 Müller, R., Grooß, J.-U., Lemmen, C., Heinze, D., Dameris, M., and Bodeker, G.: Simple measures of ozone depletion in the polar stratosphere, Atmos. Chem. Phys., 8, 251–264, https://doi.org/10.5194/acp-8-251-2008, 2008.

Pitts, M. C., Thomason, L. W., Poole, L. R., and Winker, D. M.: Characterization of Polar Stratospheric Clouds with spaceborne lidar: CALIPSO and the 2006 Antarctic season, Atmos. Chem. Phys., 7, 5207–5228, doi:10.5194/acp-7-5207-2007, 2007.

Pommereau, J.-P., Goutail, F., Lefèvre, F., Pazmino, A., Adams, C., Dorokhov, V., Eriksen, P., Kivi, R., Stebel, K., Zhao, X., and van
15 Roozendael, M.: Why unprecedented ozone loss in the Arctic in 2011? Is it related to climate change?, Atmos. Chem. Phys., 13, 5299–5308, https://doi.org/10.5194/acp-13-5299-2013, 2013.

Prinn, R. G., Weiss, R. F., Fraser, P. J., Simmonds, P. G., Cunnold, D. M., Alyea, F. N., O'Doherty, S., Salameh, P., Miller, B. R., Huang, J., Wang, R. H. J., Hartley, D. E., Harth, C., Steele, L. P., Sturrock, G., Midgley, P. M., and McCulloch, A.: A history of chemically and radiatively important gases in air deduced from ALE/GAGE/AGAGE, J. Geophys. Res., 105, 17751–17792, 2000.

20 Randel, W., Wu, F., Oltmans, S., Rosenlof, K., and Nedoluha, G.: Interannual changes in stratospheric water vapor and correlations with tropical tropopause temperatures, J. Atmos. Sci., 61, 2133–2148, 2004.

Randel, W., Wu, F., Vömel, H., Nedoluha, G. E. and Forster, P.: Decreases in stratospheric water vapor after 2001: Links to changes in the tropical tropopause and the Brewer–Dobson circulation, J. Geophys. Res., 111, D12312, doi:10.1029/2005JD006744, 2006.

Revell, L. E., Bodeker, G. E., Huck, P. E., Williamson, B. E., and Rozanov, E.: The sensitivity of stratospheric ozone changes through the
25 21st century to N_2O and CH_4, Atmos. Chem. Phys., 12, 11309–11317, https://doi.org/10.5194/acp-12-11309-2012, 2012.

Revell, L. E., Stenke, A., Rozanov, E., Ball, W., Lossow, S., and Peter, T.: The role of methane in projections of 21st century stratospheric water vapour, Atmos. Chem. Phys., 16, 13067–13080, doi:10.5194/acp-16-13067-2016, 2016.

Rex, M., Salawitch, R. J., von der Gathen, P., Harris, N. R. P., Chipperfield, M. and Naujokat, B.: Arctic ozone loss and climate change, Geophys. Res. Lett., 31, L04116, doi:10.1029/2003GL018844, 2004.

30 Rex, M., Salawitch, R. J., Deckelmann, H., von der Gathen, P., Harris, N. R. P., Chipperfield, M. P., Naujokat, B., Reimer, E., Allaart, M., Andersen, S. B., Bevilacqua, R., Braathen, G. O., Claude, H., Davies, J., De Backer, H., Dier, H., Dorokhov, V., Fast, H., Gerding, M., Godin-Beekmann, S., Hoppel, K., Johnson, B., Kyrö, E., Litynska, Z., Moore, D., Nakane, H., Parrondo, M. C., Risley, A. D., Skrivankova, P., Stübi, R., Viatte, P., Yushkov, V., and Zerefos, C.: Arctic winter 2005: Implications for stratospheric ozone loss and climate change, Geophys. Res. Lett., 33, l23808, 2006.

35 Riese, M., Ploeger, F., Rap, A., Vogel, B., Konopka, P., Dameris, M., and Forster, P.: Impact of uncertainties in atmospheric mixing on simulated UTLS composition and related radiative effects, J. Geophys. Res., 117, D16305, doi:10.1029/2012JD017751, 2012.

Rosenlof, K. H., Oltmans, S. J., Kley, D., Russell III, J. M., Chiou, E.-W., Chu, W. P., Johnson, D. G., Kelly, K. K., Michelsen, H. A., Nedoluha, G. E., Remsberg, E. E., Toon, G. C., and McCormick, M. P.: Stratospheric water vapor increases over the past half-century, Geophys. Res. Lett., 28, 1195–1198, 2001.

Sagi, K., Pérot, K., Murtagh, D., and Orsolini, Y.: Two mechanisms of stratospheric ozone loss in the Northern Hemisphere, studied using data assimilation of Odin/SMR atmospheric observations, Atmos. Chem. Phys., 17, 1791–1803, doi:10.5194/acp-17-1791-2017, 2017.

Salmi, S.-M., Verronen, P. T., Thölix, L., Kyrölä, E., Backman, L., Karpechko, A. Yu., and Seppälä, A.: Mesosphere-to-stratosphere descent of odd nitrogen in February–March 2009 after sudden stratospheric warming event, Atmos. Chem. Phys., 11, 4645–4655, 2011.

Sander, S. P., Abbatt, J., Barker, J. R., Burkholder, J. B., Friedl, R. R., Golden, D. M., Huie, R. E., Kolb, C. E., Kurylo, M. J., Moortgat, G. K., Orkin, V. L., and Wine, P. H.: Chemical Kinetics and Photochemical Data for Use in Atmospheric Studies, Evaluation No. 17, JPL Publication 10-6, Jet Propulsion Laboratory, Pasadena, USA, 2011.

Schoeberl, M. R., Dessler, A. E., and Wang, T.: Simulation of stratospheric water vapor and trends using three reanalyses, Atmos. Chem. Phys., 12, 6475–6487, doi:10.5194/acp-12-6475-2012, 2012.

Shindell, D. T., and V. Grewe: Separating the influence of halogen and climate changes on ozone recovery in the upper stratosphere, J. Geophys.Res., 107(D12), 4144, doi:10.1029/2001JD000420, 2002.

Simmons, A. J., Untch, A., Jakob, C., Kållberg, P., and Undén, P.: Stratospheric water vapour and tropical tropopause temperatures in ECMWF analyses and multi-year simulations, Q. J. Roy. Meteorol. Soc., 125, 353–386, 1999.

Sinnhuber, B.-M., G. Stiller, R. Ruhnke, T. von Clarmann, S. Kellmann, and J. Aschmann: Arctic winter 2010/2011 at the brink of an ozone hole, Geophys. Res. Lett., 38, L24814, doi:10.1029/2011GL049784, 2011.

Smalley, K. M., Dessler, A. E., Bekki, S., Deushi, M., Marchand, M., Morgenstern, O., Plummer, D. A., Shibata, K., Yamashita, Y., and Zeng, G.: Contribution of different processes to changes in tropical lower-stratospheric water vapor in chemistry–climate models, Atmos. Chem. Phys., 17, 8031–8044, https://doi.org/10.5194/acp-17-8031-2017, 2017.

Solomon, S., Garcia, R. R., Rowland, F. S., and Wuebbles, D. J.: On the depletion of Antarctic ozone, Nature, 321, 755–758, 1986.

Stenke, A., and V. Grewe: Simulation of stratospheric water vapor trends: impact on stratospheric ozone chemistry, Atmos. Chem. Phys., 5, 1257–1272, 2005.

Tegtmeier, S., Rex, M., Wohltmann, I. and Krüger, K.: Relative importance of dynamical and chemical contributions to Arctic wintertime ozone, Geophys. Res. Lett., 35, L17801, doi:10.1029/2008GL034250, 2008.

Thölix, L., Backman, L., Kivi, R., and Karpechko, A. Yu.: Variability of water vapour in the Arctic stratosphere, Atmos. Chem. Phys., 16, 4307–4321, doi:10.5194/acp-16-4307-2016, 2016.

Tian, W. S., Chipperfield, M. P., and Lü, D. R.: Impact of increasing stratospheric water vapor on ozone depletion and temperature change. Adv. Atmos. Sci., 26(3), 423–437, doi:10.1007/s00376-009-0423-3, 2009.

Vogel, B., Feck, T. and Grooß, J.U.: Impact of stratospheric water vapor enhancements caused by CH_4 and H_2O increase on polar ozone loss, J. Geophys. Res., 116, D05301, doi:10.1029/2010JD014234, 2011.

Wohltmann, I., Wegner, T., Müller, R., Lehmann, R., Rex, M., Manney, G. L., Santee, M. L., Bernath, P., Sumińska-Ebersoldt, O., Stroh, F., von Hobe, M., Volk, C. M., Hösen, E., Ravegnani, F., Ulanovsky, A., and Yushkov, V.: Uncertainties in modelling heterogeneous chemistry and Arctic ozone depletion in the winter 2009/2010, Atmos. Chem. Phys., 13, 3909–3929, doi:10.5194/acp-13-3909-2013, 2013.
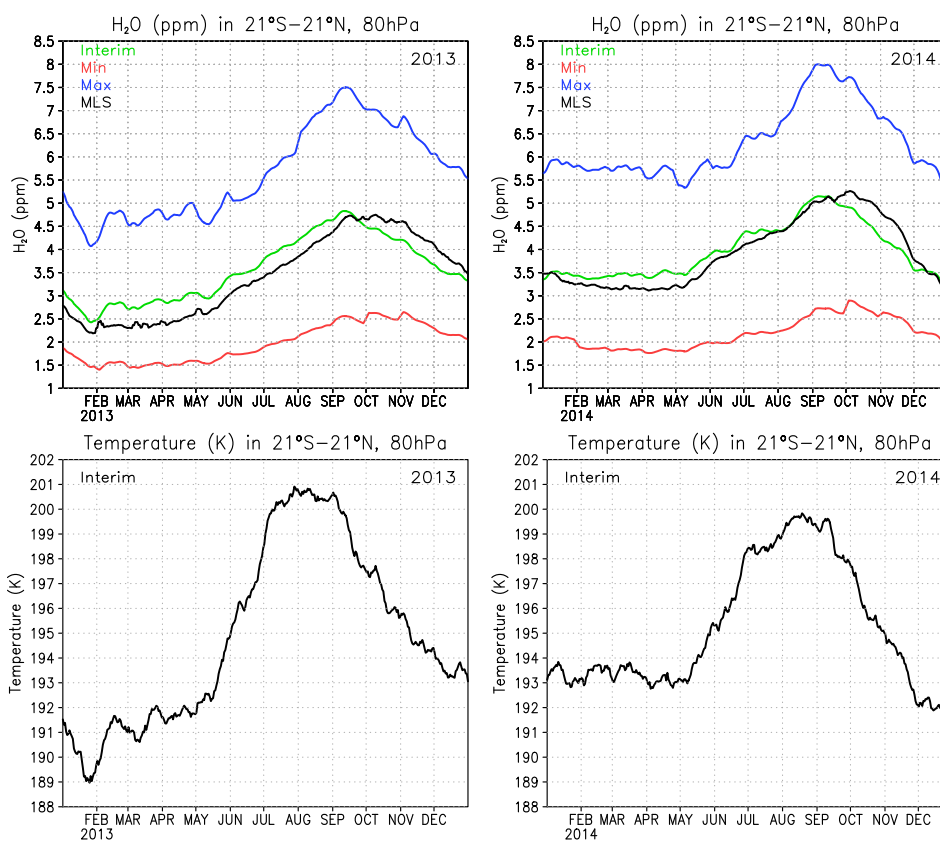
Figure 1. Water vapour and temperature around the tropical tropopause between $21°$ S and $21°$ N at level $80\,\text{hPa}$ in 2013 and 2014. Green line is Interim, blue Max, red Min simulation and black is MLS.
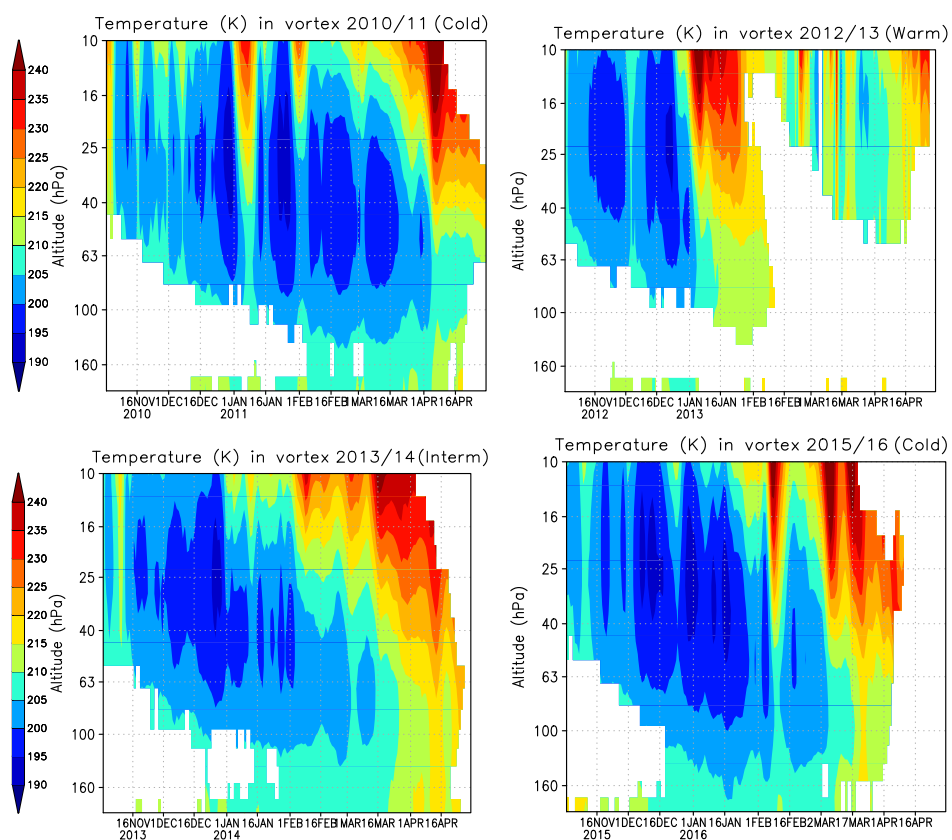
Figure 2. Vortex average temperature within the Arctic polar vortex between altitudes 170 and 10 hPa.
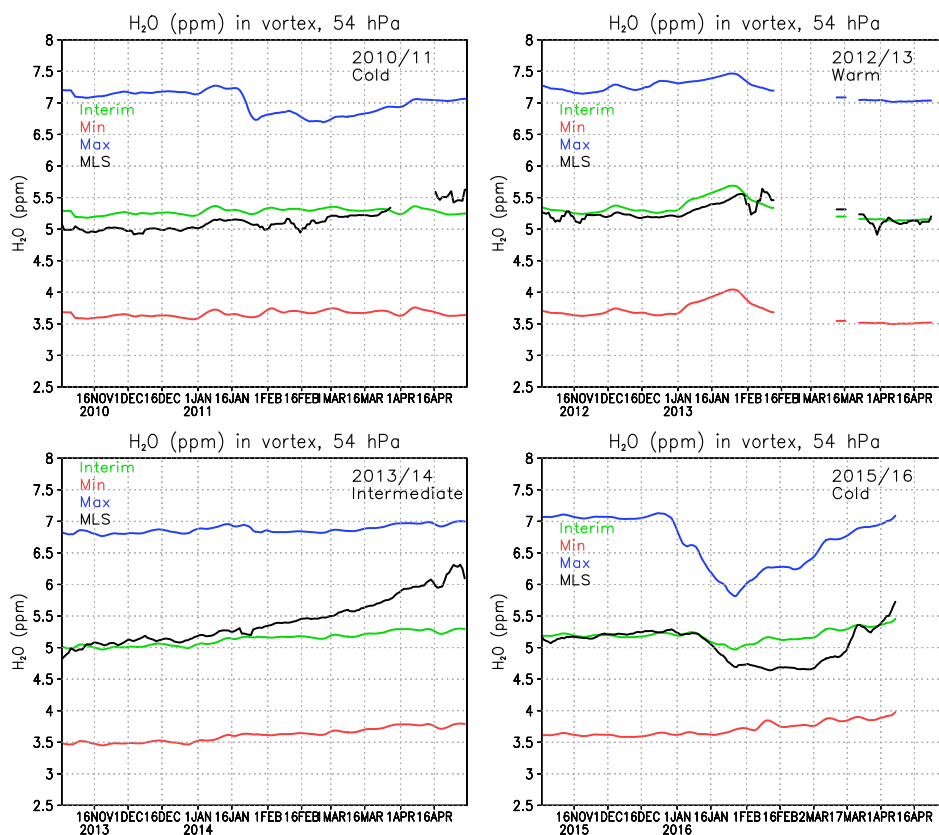
Figure 3. Water vapour concentration (ppm) at 54 hPa within the Arctic polar vortex. Green line is Interim, blue Max, red Min simulation and black is MLS.
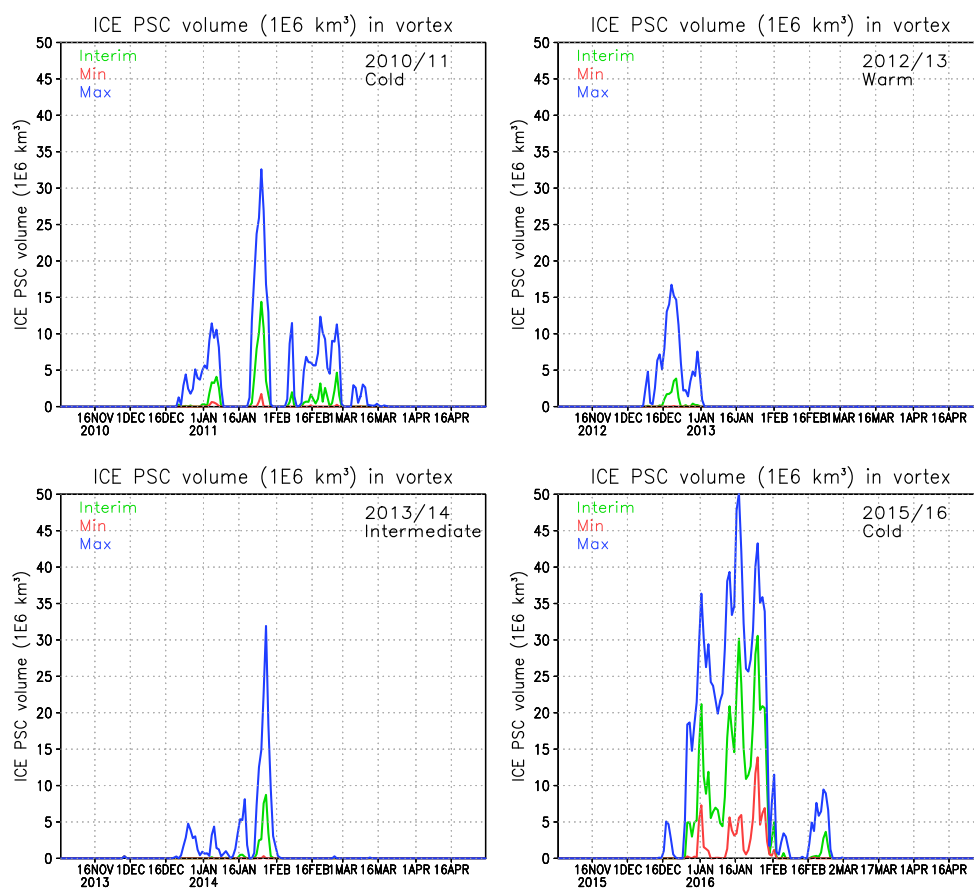
Figure 4. The volume of ICE PSCs (10^6 km^3) within the Arctic polar vortex in the FinROSE simulations. The volume is calculated between altitudes 15 and 37 km. Green line is Interim, blue Max and red Min simulation.
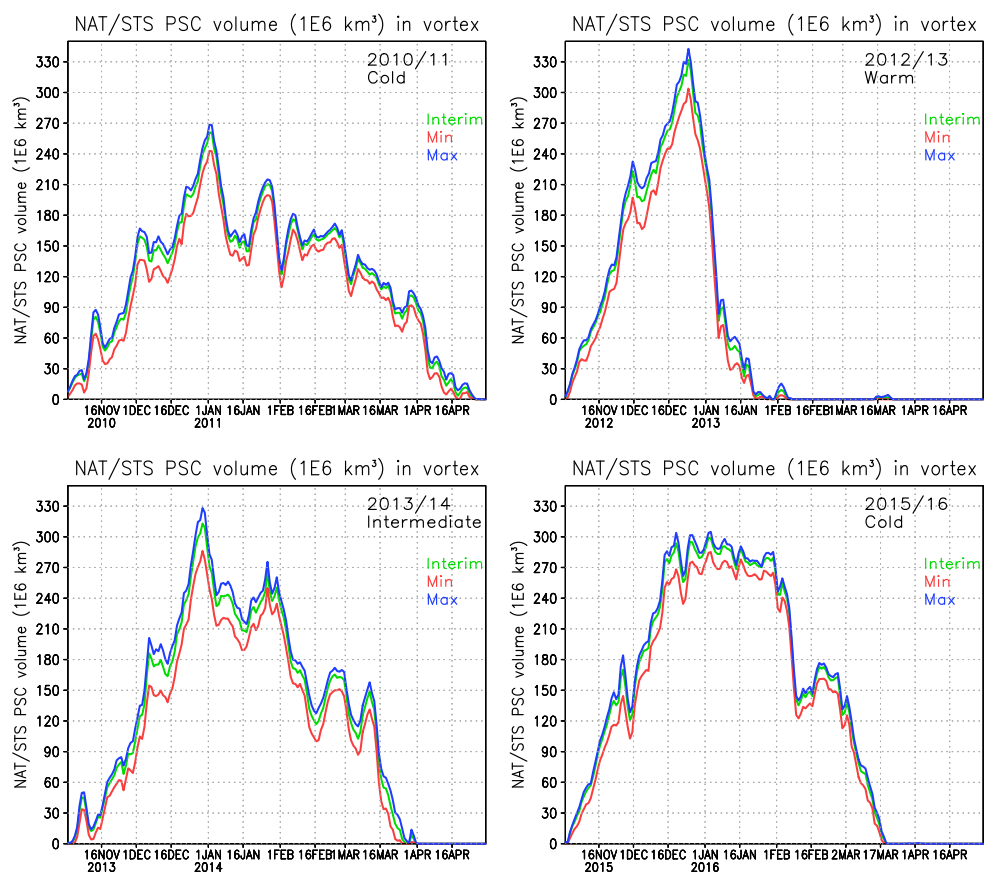
Figure 5. The volume of combined NAT and STS PSCs ($10^6 \, \mathrm{km}^3$) within the Arctic polar vortex in the simulations between altitudes 15 and 37 km. Green line is Interim, blue Max and red Min simulation.
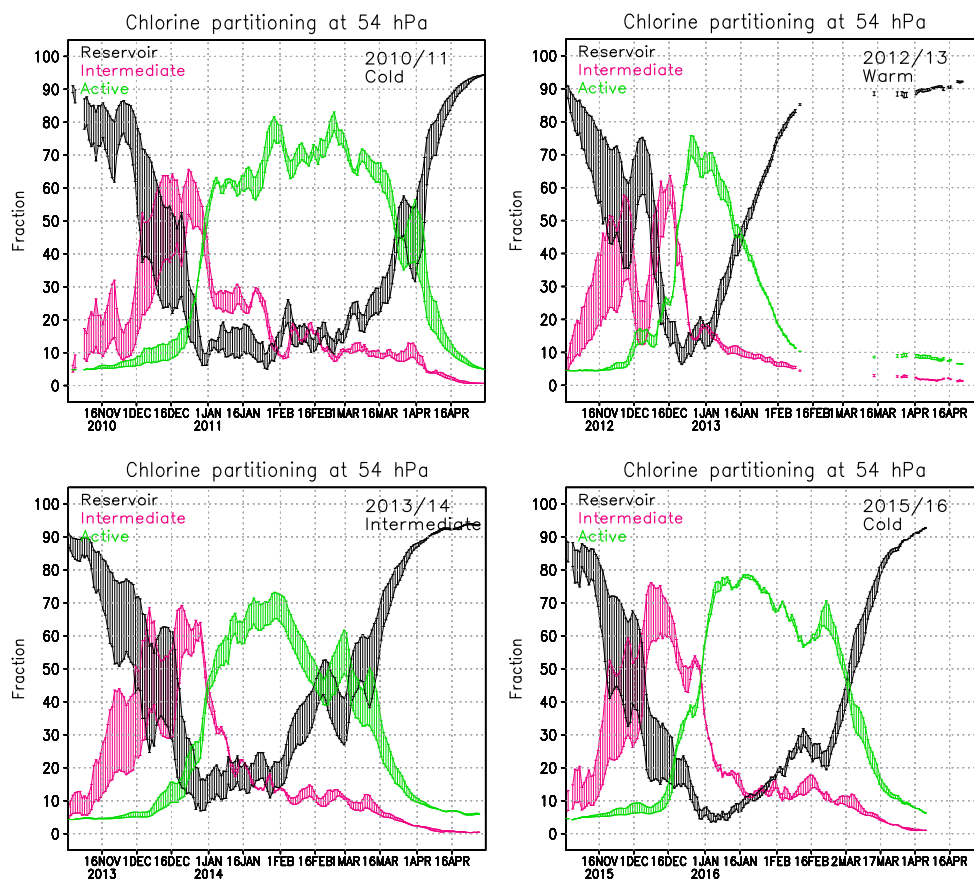
Figure 6. Chlorine partitioning (%) within the Arctic polar vortex at $54\,\mathrm{hPa}$ in the Min and Max simulations. Active form (green) is $Cl+ClO+2*Cl_2O_2$. Intermediate (magenta) contains $2*Cl_2+HOCl+OClO+BrCl+ClNO_2$ and reservoir chlorine (black) $HCl+ClONO_2$.
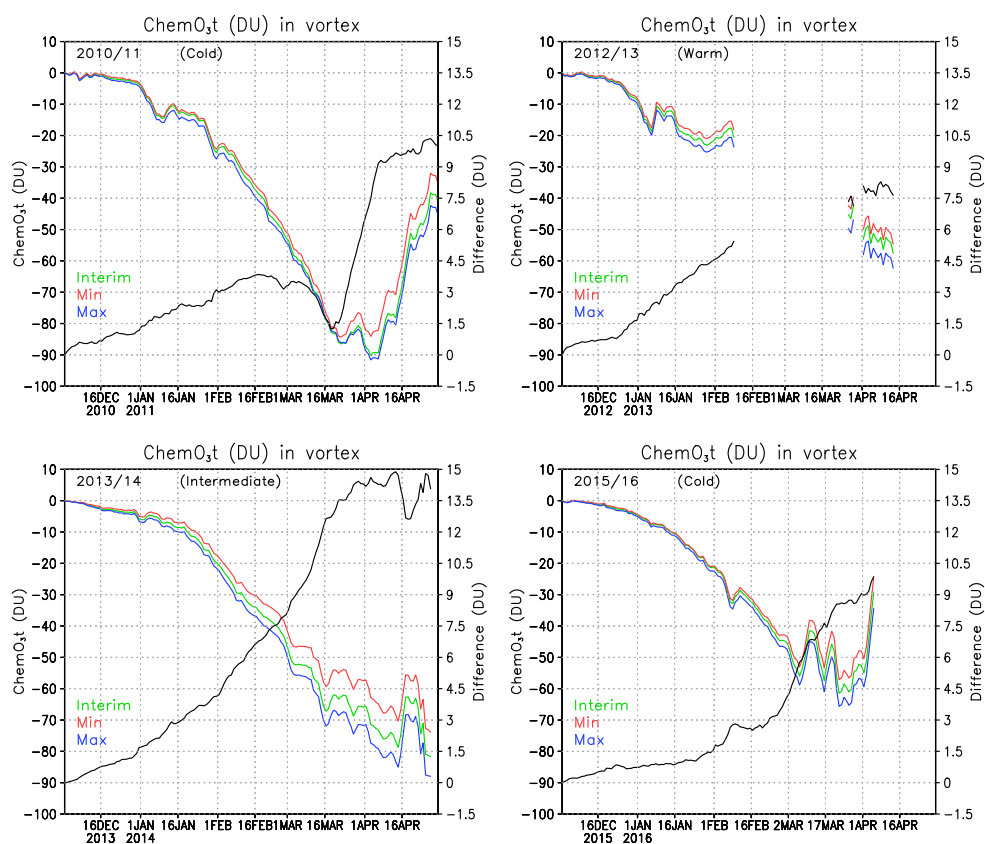
Figure 7. Chemical total ozone loss (DU) and difference between ozone loss in the Min and Max simulations within the Arctic polar vortex. Green line is Interim, blue Max and red Min simulation. The difference is in black.
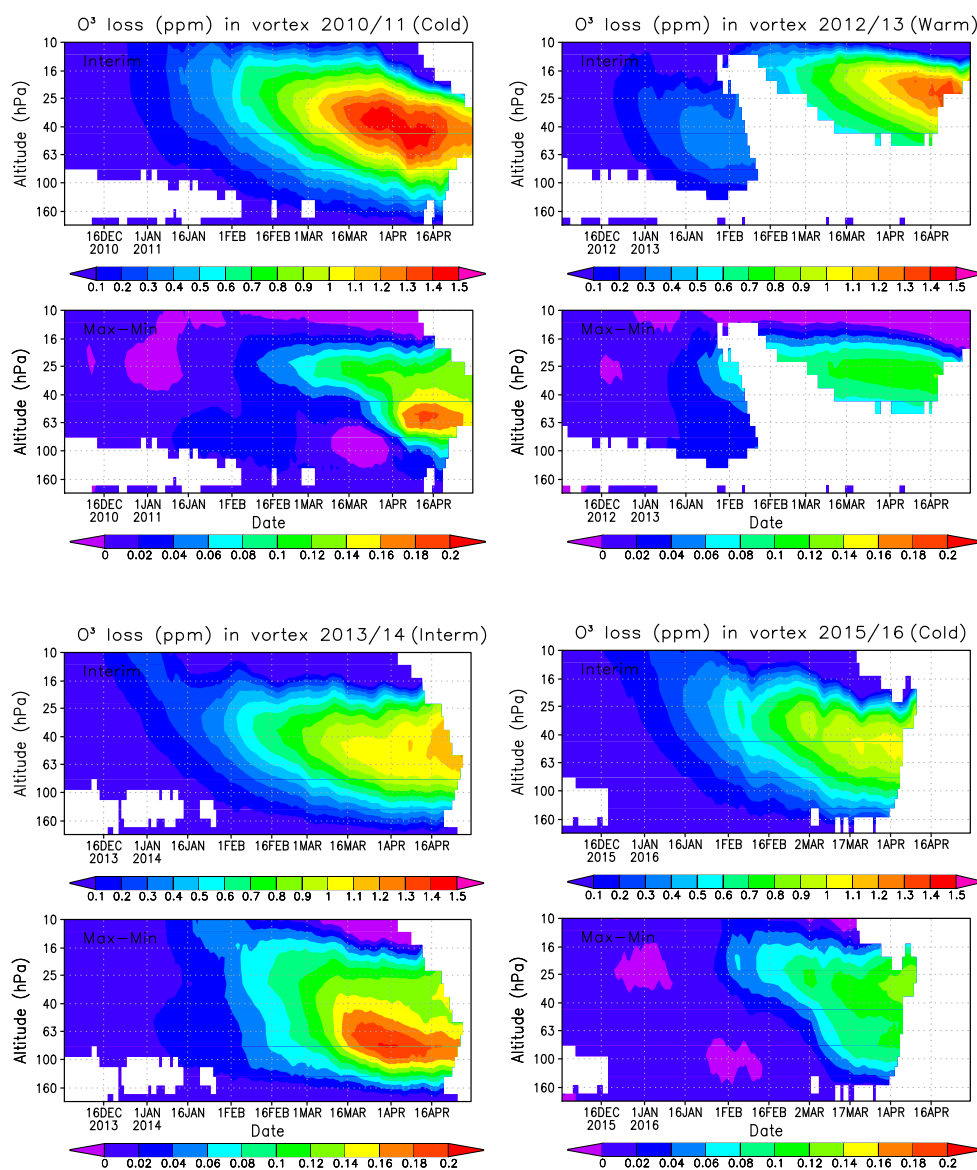
Figure 8. Averaged chemical ozone loss (ppm) in the Interim simulation (upper panels) and the difference between Max and Min simulations (lower panels) within the Arctic polar vortex.